Influence of PAN-based carbon fibres surface properties on the interfacial bonding to a phenolic matrix.

Pierre BAUDRY[1], René PAILLER[1], Marie-Anne DOURGES[1], Christine LABRUGERE[2]

[1]Laboratoire des Composites Thermo-Structuraux, 3 Allée de la Boétie, 33600 PESSAC, France
e-mail : baudry@lcts.u-bordeaux.fr Tel (+033) 556844732 Fax : (+033) 556841225
[2]Centre de Caractérisation des Matériaux Avancés, ICMCB, 87 av. A. Schweitzer, 33608 PESSAC

Abstract
This study reports an attempt to correlate ex-PAN carbon fibres surface and their interfacial properties to a phenolic matrix. The fibre surface properties were modified through chemical and thermal treatment. Atomic and functions surface contents were investigated by X-ray photoelectron spectroscopy (XPS). Surface roughness at fibre and lower scales were measured using atomic force microscopy (AFM). The single filament fragmentation test was performed on bi-matrix specimen and monitored with acoustic emission detection to measure carbon fibre/phenolic resin interfacial shear strength (IFSS). So far, results indicate a dependence between surface roughness and IFSS, while no obvious influence of surface chemistry has been found.

Introduction

Carbon fibres reinforced phenolic matrix composites are used in aerospace industry as carbon-carbon precursors due to their high char yield and suitable ablative behaviour during utilization. Nose cones or re-entry shields produced by this route exhibit appropriate thermo-mechanical properties for thermo-structural applications. The consequences of the fibres mechanical performances on the reinforced composite properties have been known for a long time [1]. The major influence of the interfacial bonding nature and intensity on the materials mechanical behaviour has been established [2]. Many studies have been carried out in order to fit the chemical component of this carbon fibre/organic matrix adhesion by treating fibre surfaces [3]. The mechanical interlocking taking place between fibres and matrix is also surmised to contribute in some cases to interfacial adhesion, and to depend on carbon fibre surface morphology [4-7]. The relative contributions of mechanical interlocking and chemical bonding to interfacial properties could depend on fibre and matrix properties.
In the present study, two commercial ex-PAN carbon fibres have undergone chemical or thermal treatments to modify their surface properties. The mechanical behaviour, the surface morphology of the untreated and treated fibres, and their surface chemical composition as well are being investigated. The effects of the applied treatments on fibres properties are depicted and allow to identify the origin of surface carbon functional distribution. The fibres roughness and chemical surface content are eventually correlated to interfacial shear stress measurements in a phenolic matrix.

Experimental

Materials

Two types of ex-PAN commercial carbon fibres have been purchased. The first one (C1) is sized to enhance its adhesion to organic matrices. The second one (C2) is not submitted to this industrial treatment. The fibres surfaces were submitted either to 50% or 100% run-time methanol cleaning to highlight the consequences of respective removal of surface pollution and sizing. Thermal treatment was achieved on C1 fibre to compare consequences on surface properties. The fibres (Figure 1) will subsequently further be referred to as: C1-m and C1-mi (industrially sized and respectively 50% or 100% methanol desized), C2-m and C2-mi (standard respectively 50% or 100% methanol washed) and C1-t (industrially surface treated and high temperature treated). The Toray T300 fibre is studied as reference too.

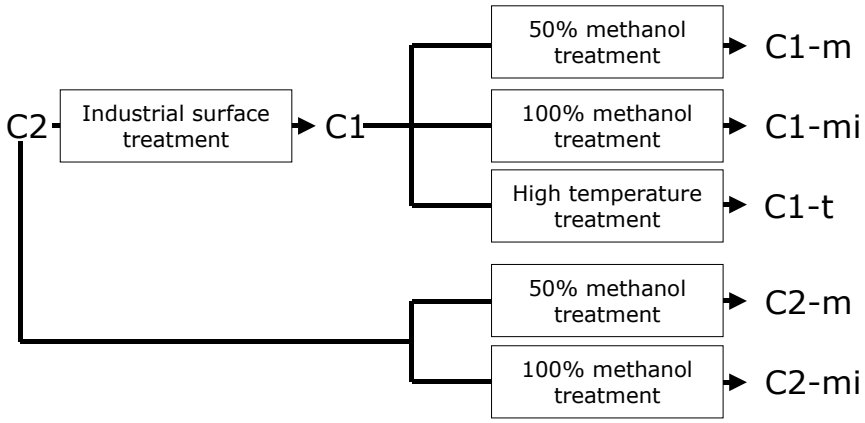

Figure 1: Fibres surface treatments.

Fibres surface characterisation

The monotonic tensile behaviour of monofilament was tested on 10 millimetres gauge length samples with a strain speed of 0.05 mm/min, and associated to Weibull statistic data treatment.

The surface morphology at fibres scale is examined using scanning electronic microscopy (SEM, Hitachi - S4500).

Surface roughness analysis was performed using atomic force microscopy (AFM, D.I. - Nanoscope III) on tapping mode. The analysed surface areas consisted in 1x1 μm^2 zones centred on the fibre. The average surface roughness is defined as

$$R_a = \int_x \int_y \left| Z_{(x,y)} - Z_0 \right| dxdy \text{ where } Z_0 = \frac{1}{x_a y_a} \int_x \int_y Z(x,y) dxdy \text{ and } x_a = y_a = 100nm .$$

A statistical probe of 10 data is processed on 100x100 nm areas centred on the fibre top: this method allows to keep the analyzed surface perpendicular to the tip, and to neglect the contribution of the fibre surface curve to R_a. No surface plane fitting or correction is needed.

X-ray photoelectron spectroscopy (XPS, V.G. – 220i-XL) results are obtained from 3 different samples for each fibre. The binding energy of core electrons emitted by surface atoms during X-ray irradiation may be deducted from their measured kinetics energy. The binding energy is dependent on the origin atomic species, and also on the bonding of this origin atom to atoms modifying its nuclear charge. As a consequence, electrons emitted by a carbon atom narrowed by electronegative species such as oxygen may have higher binding energy than electrons from a carbon atom whose nuclear charge remains unshielded. Signals of variously bonded carbon C1s can be identified with high-resolution instruments, and the amount of each C1s type may be calculated through data processing and deconvolution of overlapping peaks. It has been suggested to consider shifts to main C1s signal rather than absolute binding energy [8]. Moreover, authors [8-11] usually agree on following binding energies: C1s signal (284.6 eV) may be deconvoluated into Sp2 (284.3 eV) and Sp3 (284.8 eV), phenol and ether C-O (286.0 to 286.4 eV), carbonyl C=O (287.3 to 288.0 eV), carboxyl COOH and COOR (288.7 to 289.8). Second range carbons (C-C0) are recorded with a 285.45 eV binding energy. As the fibres are handled in ambient air and for some of them in solvent, a contribution of surface pollution to the Sp3 and C-O signals has to be taken into account.

Interfacial properties

The single fibre fragmentation test (SFFT) performed on fibres embedded in an organic matrix is a classical method to estimate the interfacial shear strength (IFSS) of these composites [12,13]. The progressive fibre fragmentation occurs in the tensile loaded specimen until the fibre fragments are too short to further fracture: this critical length l_c is obtained at saturation, and a ductile matrix is needed to reach this state. Bi-matrix fragmentation test

(BMFT) has been set up to measure the IFSS of fibre/matrix system involving a brittle matrix [13-15]: the fibre is coated with a thin sheath of the investigated brittle matrix (BM) and then embedded in a ductile support matrix (DM) dog-bone coupon. The DM prevents the BM fractures to cause failure of complete specimen. Modelling and experimental researches [16] report that fractures in BM occur during BMFT but do not affect the stress transfer in the bimatrix system. Unless the DM fails before saturation, the Kelly-Tyson stress analysis [17] can be used to calculate the IFSS:

$$\tau = \frac{r_f \sigma_c}{l_c}$$

where r_f is the fibre radius, σ_c the tensile strength of the fibre at critical length l_c. Assuming a Weibull distribution [18,19], the fibre ultimate tensile strength σ_c is related to tensile strength σ_0 at gauge length l_0 and to Weibull modulus m by:

$$\frac{\sigma_0}{\sigma_c} = \left(\frac{l_c}{l_0}\right)^{1/m}$$

The critical length l_c can be deducted from:

$$l_c = \frac{1}{K}\bar{l}$$

where K is estimated [20] equal to 0.75. More complex models have been established to process data supplied by fragmentation test, and reviewed [21]. The influence of DM on results has also been established and some normalization methods have been proposed [22]. As the mechanical properties and Weibull parameters of studied fibres are similar, the Kelly-Tyson model is considered to compare IFSS values.

The acoustic emission detection (AE) [23] is a suitable non-destructive testing method to monitor the fragmentation of fibres embedded in opaque resins. The different acoustic events occurring during the tensile testing of single-fibre bimatrix specimen are recorded and discriminated through Fourier transform spectral analysis [24]. The fibre failures are counted and located through the use of two captors. This monitoring is validated by a transmission optic microscopy study of the fibre ruptures in a sample.

Carbon fibres are embedded in a thin phenolic resin sheath and centred in a dog-bone epoxy specimen [25]. The probe are tensile loaded (0.05 mm/min, Instron 4505) to saturation and the acoustic activity is recorded (Mistras 2001). Data processing is carried out on 10 samples per fibre.

Results and discussion

Morphological and mechanical properties of the fibres.

SEM analyses supply fibre diameter measurement but do not allow to differentiate the studied ex-PAN carbon fibres surface morphology, as seen on Figure 2 (a-c). All the fibres exhibit surface striations attributed to polymer spinning during elaboration.

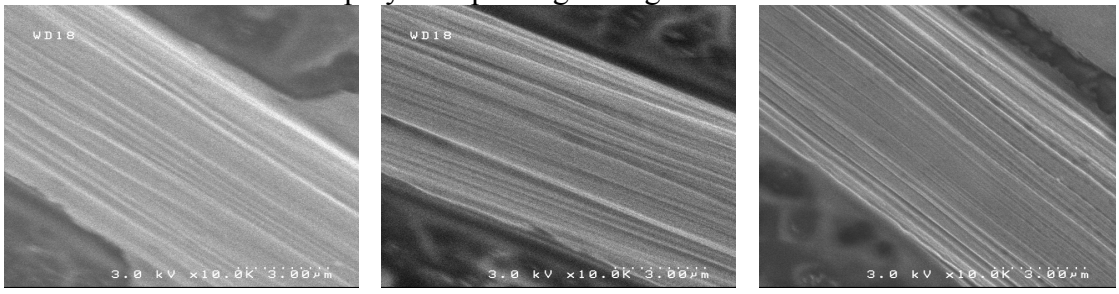

Figure 2: SEM analyses of (a) T300, (b) C1 and (c) C2 fibres.

Tensile test results on fibres are listed in Table 1, including Young's modulus E_0, tensile strength σ_r, rigidification factor f [26] and Weibull modulus m.

Table 1: fibre tensile test data

Fibres	Valid samples	Mean diameter d (μm)	Young's modulus E_0 (Gpa)	Rigidification factor f (E= E_0(1+f.ε))	Strength σ_R (Pr=0.5) (Mpa)	Weibull modulus m
C2	23	7.0±0.2	248 ±15	~11	3523 ±204	6.1
C2-m(*)	17	7.0±0.2	251 ±15	~11	3734 ±214	6.9
C1	17	7.0±0.2	246 ±15	~11	3573 ±207	6.1
C1-m(*)	21	7.0±0.2	245 ±15	~11	3580 ±207	6.2
C1-t	>10	7.0±0.2	253 ±16	~21	3050 ±650	5.0
T300	>10	7.0±0.2	222 ±14	~12	2369 ±144	7.6

(*) No significant difference was found between C2-m and C2-mi, neither between C1-m and C1-mi.

The sizing and the chemical treatment do not affect the mechanical properties of the fibres. As mentioned in the literature, the high temperature treatment of the C1 fibre enhances its stiffness [27], and reduces its Weibull modulus as the consequence of the creation of defects.

X-ray photoelectron spectroscopy.

Binding energy values of deconvoluated peaks (Table 2) agree with former studies [8-11].

Table 2. XPS results: fibre surface element content and C1s functional distribution.

Fibre	Element content (%)			Relative atomic distribution (%) and binding energy (eV) of C1s functional groups					
	C1s	**O1s**	**residue**	**Sp2**	**Sp3**	**C-CO**	**C-O**	**C=O**	**COOR**
C1	81.6	15.9	2.5 (N)	22.36	35.17	9.20	25.22	3.47	4.58
				284.37 eV	*284.93 eV*	*285.41 eV*	*286.43 eV*	*287.43*	*288.84 eV*
C1-m	84.3	11.9	2.6 (N)	23.72	35.79	19.94	12.39	1.96	6.20
			1.2 (Si)	*284.17 eV*	*284.70 eV*	*285.47 eV*	*286.43 eV*	*287.43 eV*	*288.55 eV*
C1-mi	90.0	10.0		48.09	32.69	4.30	11.27	3.65	
				284.30 eV	*284.90 eV*	*285.41 eV*	*286.34 eV*	*287.56 eV*	
C1-t	92.6	7.4		47.13	30.45	9.60	8.77	1.79	2.26
				284.18 eV	*284.72 eV*	*285.46 eV*	*286.39 eV*	*287.39 eV*	*288.39 eV*
C2	79.3	18.4	2.3 (Na)	18.04	32.84	20.75	22.48	18.49	1.89
				284.22 eV	*284.84 eV*	*285.52 eV*	*286.40 eV*	*287.53 eV*	*288.48 eV*
C2-m	89.5	9.1	1.4 (Na)	32.62	36.32	16.08	10.23	4.09	0.66
				284.18 eV	*284.68 eV*	*285.45 eV*	*286.34 eV*	*287.34 eV*	*288.43 eV*
C2-mi	94.0	6.0		56.03	8.88	19.90	12.64	2.55	
				284.30 eV	*284.90 eV*	*285.41 eV*	*286.58 eV*	*287.56 eV*	
T300	70.9	22.5	3.8 (N)	21.90	27.46	14.85	27.81	5.77	2.21
			3.6 (Si)	*284.48 eV*	*285.04 eV*	*285.47 eV*	*286.44 eV*	*287.44 eV*	*288.48 eV*

The methanol washing of both C1 and C2 fibres causes a decrease in surface oxygen content and the removal of residual hetero-atoms. The high temperature treatment performed on C1 fibre provides lower oxygen content than the 100% desizing with methanol. The surface oxygen content is the highest for T300, medium for C2, and the lowest for C1 fibre.

On the fibres treated with methanol, C-O and sp3 signals drop as a consequence of surface pollution removal. The washing of C2 surface reveals its sp2-hybridized structure with C-O and C=O functions. The 50% run-time chemical desizing of C1 fibre with methanol (C1-m) causes a partial elimination of the sizing. This coating may consist in carboxylic polymeric chains and phenoxy groups. After a 100%-run time methanol treatment (C1-mi) the surface

carbon atoms are mainly sp2 hybridized. The distributions of C1s functional groups on this fibre surface and on high temperature treated fibre C1-t are close.

Atomic force microscopy

As the measured areas are located between the usual spinning striations found on ex-PAN carbon fibres, the average roughness values proposed in Table 3 are representative of the small scale morphology of the fibres. Analyses performed at larger scale ($1x1\mu m^2$) are in good agreement with other AFM [7,28] and STM [29] recordings described in the literature.

Table 3: AFM roughness analysis on 100x100 nm^2 areas.

Fibre	Average surface roughness Ra (nm) ±0.01
C1	3.30
C1-m	1.09
C1-mi	0.83
C1-t	2.14
C2	1.63
C2-m	1.72
C2-mi	2.09
T300	1.61

The high surface roughness of C1 fibre decreases as the sizing is removed by chemical treatment. The desizing by high temperature treatment creates a less regular surface than the chemical washing. A close processing of AFM captures reveals the morphology of the polymeric sizing on C1 fibre. The polymeric ~50nm-wide network of deposited coating on C1 fibre (Figure 2-b) fits the boundaries of the nodular structure found on C2 carbon surface by relief enhancement (Figure 2-a). The initial sizing of C1 is carbonized at high temperature, but remains as residue on the fibre (Figure 2-c). This carbonized residue is located at the junctions of the emerging nodular structure. The nodules could correspond to more organized areas whose borders are plan edge-rich zones. These borders are known to be more oxidized and thus oxygen richer zones. The polymeric sizing rather deposits on these borders, creating an asperity network and a high surface roughness.

The partial chemical treatment does not modify the surface morphology of C2 fibre, but complete treatment enhances its roughness. This may be due to removal of pollution or elaboration residues liberating access to surface porosity.

The average surface roughness is lower for C1-mi than for C2 fibre: AFM monitoring of methanol treatment on C1 fibre shows that the sizing attack by the solvent is not homogeneous and provides smooth C1-m and C1-mi surfaces. The polymeric asperities are first solved and it results in a surface levelling. Even with 100% run time methanol desizing, polymeric residues may subsist in crevices and create a smooth surface.

The sizing and the way it is removed (by solvent or high temperature treatment) have consequences on fibres surface morphology and small scale surface roughness.

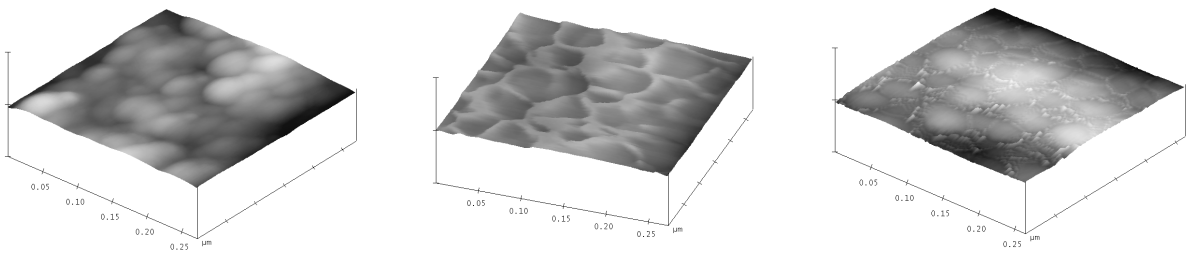

Figure 3: AFM captures (~250x250 nm^2, relief enhanced by color treatment) of (a) C2, (b) C1 and (c) C1-t

Interfacial shear strength testing
Results are presented in Table 4.

Table 4: IFSS data supplied by BMFT and processed with Kelly-Tyson model.

Fibre	IFSS (MPa)
C1	38 ± 5
C2	26 ± 5
T300	27 ± 5

The interfacial shear strength to a phenolic matrix is very close for the C2 and T300 fibres, and higher for the C1 fibre. The O1s/C1s atomic ratio of C2 (0,23) and T300 (0.32) are different and the fibre developing the higher interaction with the phenolic matrix shows the lower O/C surface ratio (C1: 0.19). The surface oxygen content of this type of fibres can obviously not be directly correlated with interfacial shear strength. If the chemical functions of the C1 and C2 fibres are considered, the major difference in IFSS should be attributed to the COOR functions and/or to the presence of 2.5% N on the C1 surface. To raise fibre/matrix adhesion, the coating polymer has to be reactive to both fibre surface and phenolic resin, and in a greater extent than the fibres to the phenolic matrix. That can be achieved through the introduction of amino groups. Amino groups are known to be very reactive to organic resins, but the presence of N on T300 fibre does not raise the IFSS to the investigated phenolic matrix. The boundary zones found on C2 fibre and revealed after the removing of C1 coating, either by thermal and chemical treatment, are supposed to be more reactive zones, considering the greater amount of organic sizing deposited on these areas. The C=O and C-O functions located in these end-of-plan rich regions could react with the coating agent.
The fibre/matrix interactions show a good dependence to the small-scale fibre surface morphology. The coating of the C1 fibre consisting in an asperities network enhances the surface roughness and results in a better mechanical interlocking with the phenolic matrix. The surface roughness, as described before, influences fiber/matrix adhesion by increasing contact surface and thus enhancing surface energy interactions and chemical bonding probability. In the particular case carried out in the present research, the determinant role of surface roughness appears to be the improvement of mechanical interlocking. This proposition is supported by the radial strain state created at the fibre/matrix interface in a carbon fibre / phenolic matrix composite, resulting from the phenolic matrix polymerisation.

Conclusion

In the present study, fibres with different surface chemistry and morphology were characterised. The surface atomic content, the carbon functionality, the average surface roughness in inter-striation zones identified as parameters influencing the fibre/matrix adhesion were investigated. Among the fibre sample examined here, no obvious influence of the surface chemistry on IFSS to a phenolic matrix was found. In the meantime, a direct dependence was noticed between the carbon fibre/phenolic matrix adhesion and the average surface roughness. The industrial surface treatment is noticed to convert a lower chemical reactivity of the original fibre in a higher mechanical interactivity. The in-progress experiments on intermediate surface treated fibres may corroborate the predominance of the mechanical interlocking contribution on surface chemical bonding for these ex-PAN carbon fibre/phenolic resin composites. The surface structure of the founded nodular morphology on fibre will also further be investigated.

The author thanks the French national committee for scientific research (CNRS), CEA and Snecma for funding and material support.

References

[1] Savage G., Carbon-Carbon Composites, London, Chapman & Hall, 1993
[2] Fitzer E., Weiss R., Carbon 25 (1987) 455-467
[3] Akihido Fukunaga, Shigetomo Ueda, Comp Sci & Technol 60 (2000) 249-254
[4] Donnet J.-B., Bansal R.C., Carbon Fibres, 2nd Edition, New York, Marcel Dekker, 1990
[5] Harvey J., Kozlowski C., Sherwood P.M.A., J. Mater. Sci. 22 (1987) 1585-1596
[6] Guigon M., J. Mater. Sci. 27 (1992) 4591-4597
[7] Drzal L.T., Sugiura N., Hook D., Composite Interfaces, Vol.4, No. 5 (1997) 337-354
[8] Papirer E., Lacroix R., Donnet JB., Carbon 32 (1994) 1341-1358
[9] Boehm H.P., Carbon 40 (2002) 145-149
[10] Dilsiz N., Wightman J.P, Carbon 37 (1999) 1105-1114
[11] Gardner S.D., He G., Pittman, Jr C.U, Carbon 34 (1996) 1221-1228
[12] Drzal LT., Mater Sci Eng 21 (1990) 289-293
[13] Favre J.P., Jacques D., J. Mater. Sci. 25 (1990) 1373-1380
[14] Chen F., Tripathi D., Jones F.R., Composites Part A, 27-A (1996) 505-515
[15] Lee S.I., Park J.M., Shin D.W., Yoon D.J., Polym Comp 20 (1999) 19-28
[16] Chen F., Tripathi D., Jones F.R., Comp Sci & Technol. 56 (1996) 609-622
[17] Kelly A., TysonW.R., J. Mech. Phys. Solids 13 (1965) 329-350
[18] Khalili A., Kromp K., J. Mater. Sci. 26 (1991) 6741-6752
[19] Curtin W.A., Netravali A.N., Park J.M., J. Mater Sci 29 (1994) 4718
[20] Oshawa T. *et al.* , J. Applied Polym Sci 22 (1978) 3203
[21] Shiqiang Deng, Yiu-Wing Mai, Hong-Yuan Liu, Composites Part A, 29A (1998) 423-434
[22] Tripathi D. *et al.*, J. Matter. Sci. 32 (1997) 4759-4765
[23] Okoroafor E.U., Hill R., J. of Physics, Part D: Applied physics 28 (1995) 1816-1825
[24] Berthelot J.M., Rhazi J., Comp Sci & Technol 37 (1990) 411-428
[25] Lee S.M., Holguin S., J. Adhesion 31 (1990) 91-101
[26] Shioya M., Hayakawa E., Takaku A., J. Mater. Sci. 31 (1996) 4521-4532
[27] Sauder C., Ph-D Thesis N°2477, Univ. Bordeaux I, 2001
[28] Marieta C., Schulz E., Mondragon I., Comp Sci & Technol 62 (2002) 299-300
[29] Bouchard E., Ph-D Thesis N°2162, Univ. Bordeaux I, 1999